Structural Engineering and Mechanics, Vol. 34, No. 2 (2010) 159-174
DOI: http://dx.doi.org/10.12989/sem.2010.34.2.159

Using FEM and artificial networks to predict on elastic buckling load of perforated rectangular plates under linearly varying in-plane normal load

Mustafa Sonmez and M. Aydin Komur†

Department of Civil Engineering, Faculty of Engineering, Aksaray University, 68100 Aksaray, Turkey

(Received August 5, 2008, Accepted October 28, 2009)

Abstract. Elastic buckling load of perforated steel plates is typically predicted using the finite element or conjugate load/displacement methods. In this paper an artificial neural network (ANN)-based formula is presented for the prediction of the elastic buckling load of rectangular plates having a circular cutout. By using this formula, the elastic buckling load of perforated plates can be calculated easily without setting up an ANN platform. In this study, the center of a circular cutout was chosen at different locations along the longitudinal *x*-axis of plates subjected to linearly varying loading. The results of the finite element method (FEM) produced by the commercial software package ANSYS are used to train and test the network. The accuracy of the proposed formula based on the trained ANN model is evaluated by comparing with the results of different researchers. The results show that the presented ANN-based formula is practical in predicting the elastic buckling load of perforated plates without the need of an ANN platform.

Keywords: artificial neural networks; plate buckling; perforated plates; linearly varying loading; explicit formula.

1. Introduction

The buckling behavior of steel plates has been studied by many researchers in structural mechanics for over a century (Timoshenko 1961, Chajes 1974, Brush and Almroth 1975). Steel plates are often used as the main components of steel structures such as ship decks and hulls, platforms on oil rigs, and plate and box girders of bridges. Openings in steel plates may be required to provide access for inspection, maintenance, or simply to reduce weight. However, the presence of such openings in plate elements leads to changes in stress distribution within the member and variations in buckling characteristics of the plate element (Shanmugam *et al.* 1999).

The effects of the shape, size, location, and types of applied load on the performance and buckling behavior of such perforated plates have been investigated by several researchers over the past two decades. For example, Shanmugam *et al.* (1999) reviewed most of the previous work on the elastic buckling of perforated plates. Then they analyzed several uniaxially and biaxially loaded perforated square plates with different boundary conditions by using the finite element method

† Corresponding author, E-mail: makomur@aksaray.edu.tr

(FEM). They showed that an increase in the hole size and slenderness ratio causes a significant loss in the ultimate strength of perforated plates. Brown and his colleagues (1986, 1987, 1990) used the conjugate load/displacement method (CLDM) to investigate the parameters affecting the stability of perforated plates subjected to different types of loading. They also investigated the effects of eccentricity of a rectangular hole on the buckling of a square plate under in-plane uniaxial and shear loading. El-Sawy and Nazmy (2001) used the FEM to investigate the effect of plate aspect ratio and hole location on the elastic buckling load of rectangular plates subjected to uniaxial end compression in their longitudinal direction. They concluded that a perforated square panel that is a part of a rectangular plate cannot be treated as a separate square plate having the perforation.

Recently Komur and Sonmez (2008) investigated the effect of the plate aspect ratio and the hole location on the buckling of rectangular plates subjected to linearly varying in-plane loading. They showed that the presence of a circular hole always causes a decrease in the elastic buckling load of plates subjected to bending, even if the circular hole is not in the outer panel.

ANN has been used by many researchers for a variety of engineering applications including predicting the buckling load of beams and plates. El-Kassas *et al.* (2002) used ANN to predict the failure load of cold-formed steel compression members. They reported that the trained ANN can encapsulate complex relationships very effectively and produces results significantly quicker than using conventional methods. Pu and Meshabi (2006) used ANN to predict the ultimate strength of unstiffened plates under uniaxial compression. They indicated that the ANN method could be used to establish a functional relationship between input and output parameters. Cevik and Guzelbey (2007) presented two plate strength formulations applicable to metals with nonlinear stress–strain curves, such as aluminum and stainless steel alloys, obtained by soft computing techniques, namely ANN and genetic programming. Komur and Sonmez (2005) showed that ANN may be used to predict the elastic buckling load of rectangular perforated plates under compression.

In the literature, a great deal of attention has been focused on studying the elastic buckling of perforated plates subjected to different types of loading, but the ANN has not been applied to predict the elastic buckling load of perforated plates subjected to linearly varying in-plane loading. The objective of this paper, therefore, is to establish an ANN model based on the results obtained from the finite element method and to present a formula based on this trained ANN model predicting the elastic buckling load of plates. The use of the formula will ease the calculation of elastic buckling load of plates for engineers.

2. Linear buckling analysis

In linear elastic analysis, the stress distribution is obtained after load is applied to the model structure, but the load magnitude which the structure can sustain is unknown. In order to determine the maximum load carrying capacity of the structure, nonlinear analysis or buckling analysis must be employed. In nonlinear analysis, externally applied load is divided into smaller load steps, then these smaller loads are incrementally applied and an equilibrium state is searched through iteration. Hence, the maximum load carrying capacity or instability point(s) of the structure is determined by tracing the peak load in a load-deflection curve. The second method is the buckling analysis by which one may obtain only the critical loads and the corresponding deformation mode shapes of the modeled structure. There are two types of buckling analysis: linear and nonlinear. The linear buckling analysis (or eigenvalue analysis) is performed in two steps. The first step is an elastic

linear analysis which is performed to determine the internal stresses (initial stress) in the structure due to externally applied loads. The second step is to determine the eigenvalues based on the stiffness matrix obtained from the linear analysis. The linear buckling analysis will not be suitable if the deformations are not small or material shows nonlinear behavior near the collapse. In such cases, the nonlinear buckling analysis, which is a combination of both nonlinear analysis and linear buckling analysis, must be performed.

In the present study, the material behavior is assumed to be linear elastic and deformations compared with the overall dimensions of plate are assumed to be small. Based on the assumptions, the linear buckling analysis is used in the analysis of perforated plates.

ANSYS (2005) uses the first and second order terms of strain to generate the stiffness matrices in the buckling analysis. The first term of strain yields the conventional stiffness matrix, K_0, and the second term of strain is to account for the stress stiffness matrix, K_σ. The stress stiffness matrix, K_σ, accounting for the effects of existing stress, is proportional to the stress level in the plate. The total stiffness matrix including effect of stress σ_o can be expressed as

$$[K] = [K_0] + [K_\sigma(\sigma_0)] \tag{1}$$

Stress σ_0 at buckling is unknown at the beginning of the analysis. By applying a small load (e.g., unit load) which is proportional to the applied load to the plate, the stress at buckling reaches to the level of $\sigma_0 = \lambda\sigma_{0l}$, where λ is a scalar multiplier and σ_{0l} is the stress due to the applied small load. The stiffness matrix can be expressed as

$$[K] = [K_0] + [K_\sigma(\lambda\sigma_{0l})] = [K_0] + [K_\sigma(\sigma_{0l})] \tag{2}$$

Then the matrix equilibrium equation may be given as

$$\{F\} = ([K_0] + \lambda[K_\sigma(\sigma_{0l})])\{D\} \tag{3}$$

where $\{F\}$ and $\{D\}$ are the external load and the corresponding nodal displacement vector, respectively. At the buckling, the plate displacements increase with no increase in the external load. Mathematically, this can be defined by

$$\{F\} = ([K_0] + \lambda[K_\sigma(\sigma_{0l})])\{D\} = ([K_0] + \lambda[K_\sigma(\sigma_{0l})])\{D + dD\} \tag{4}$$

where $\{dD\}$ is the incremental nodal displacement vector. Subtraction of the first equation from the second yields

$$([K_0] + \lambda[K_\sigma(\sigma_{0l})])\{dD\} = 0 \tag{5}$$

The incremental displacement vector $\{dD\}$ cannot be zero (Cook *et al.* 1989); therefore, a non-trivial solution of Eq. (5) is

$$\det([K_0] + \lambda[K_\sigma(\sigma_{0l})]) = 0 \tag{6}$$

Calculating the determinant given in Eq. (6) gives n-different eigenvalues λ_i, where n is the dimension of stiffness matrix. The lowest eigenvalue λ_1 corresponds to the critical stress level $\lambda_1\sigma_{0l}$ where buckling occurs. The associated eigenvectors represent the characteristic mode shapes of the buckled plate.

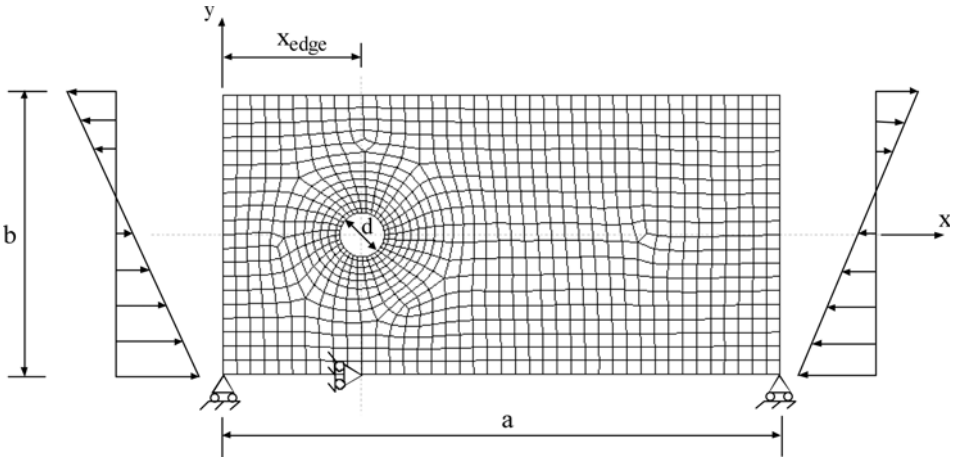

Fig. 1 Geometry and typical mesh of a plate with a circular hole

3. Finite element analysis procedure

The ANSYS shell element library includes general-purpose shell elements and specifically formulated shell elements for thick and thin shell problems. In this study, the general-purpose Elastic Shell63 element is used to model the perforated plate because it has the capacity to simulate both membrane and flexural behavior. The Elastic Shell 63 element has four nodes possessing six degrees of freedom per node. This element was selected for use in the parametric study based on its satisfactory performance in verification work previously described by El-Sawy and Nazmy (2001) and El-Sawy *et al.* (2004).

In this study an irregular mesh discretisation in finite element modeling is employed as shown in Fig. 1. The mesh density of the plate was chosen based on the size of a circular hole. The default shell element size was selected as $b/20$. The shell element size along the hole perimeter was set to the smaller of $b/50$ or $\pi d/40$. The mesh pattern was set-up on the basis of the results achieved in previous numerical studies (El-Sawy and Nazmy 2001). The center of the circular holes, located at distance x_{edge} from the nearest loaded end, was moved along the x-axis from the plate outer edge $x_{edge} = 0.05b + d/2$ toward the center of the plate ($x_{edge} = a/2$). The material of the plates was assumed to be homogeneous, isotropic and elastic with Young's modulus $E = 210$ GPa and Poisson's ratio $\upsilon = 0.3$ were selected.

4. Elastic buckling of perforated plates

A rectangular plate given in Fig. 1 has length a, width b, thickness t and a circular hole with the diameter d. The plate is subjected to linearly varying in-plane loading in the longitudinal direction and all its edges are simply supported in the out-of-plane direction. In other words, there is no lateral edge displacement perpendicular to the plate plane on all four edges. Three points on the edge at $y = -b/2$, are restrained from in-plane translation to prevent the plate from exhibiting rigid

body motion. Two of three points are restrained from translating in the y-direction and the third restraint is used to prevent an x-direction translation. The location of the third restraint is chosen at the intersection point of the plate's longitudinal edge and the section of the hole center (El-Sawy and Nazmy 2001). Plate aspect ratios (a/b) are selected to have integer values i.e., 1, 2, 3 and 4 in order to investigate the effects of the aspect ratio on the buckling load.

A linearly varying force is subjected to two opposite edges ($x = 0$ and $x = a$) as follows

$$N_x = -N_0\left(1 - \frac{\alpha}{b}\left(y + \frac{b}{2}\right)\right) \tag{7}$$

where N_o and α are the intensity of the compressive force per unit length and a numerical factor, respectively. Negative sign in Eq. (7) represents compression. By changing α in Eq. (7), different particular cases may be obtained as shown in Fig. 2. For instance, if α is set to zero, the uniformly distributed compressive force is obtained. By taking $\alpha = 1$, the compressive force varies linearly from $-N_o$ at $y = -b/2$ to zero at $y = b/2$. For $\alpha = 2$, pure in-plane bending is obtained. The other cases ($\alpha = 0.5$ and $\alpha = 1.5$) give a combination of bending and compression. Hereafter, the loading cases of $\alpha = 0.0$, 0.5 and 1.0 are called "compression," and $\alpha = 1.5$ and 2.0 are called "bending" for the sake of simplicity. The case of $\alpha < 0$ or $\alpha > 2$ are not considered because such cases are identical with the cases of $0 \le \alpha \le 2$ (Leissa and Kang 2002, Kang and Leissa 2005).

In order to verify the method of analysis used in this study, a comparison with existing results in the literature on the elastic buckling of rectangular plates without a cutout was performed. The non-dimensional buckling in-plane loads N^*_{cr} in Eq. (8) obtained by ANSYS, along with the corresponding values obtained from Kang and Leissa (2005), are listed in Table 1. They obtained these results by using an exact solution procedure based on the infinite power series. There is a good agreement between the two sets of results. The maximum deviation was less than 1% and within an acceptable level.

$$N^*_{cr} = \frac{N_o b^2}{D} \tag{8}$$

D in Eq. (8) is the flexural rigidity of the plate defined by

$$D = \frac{Et^3}{12(1-\nu^2)} \tag{9}$$

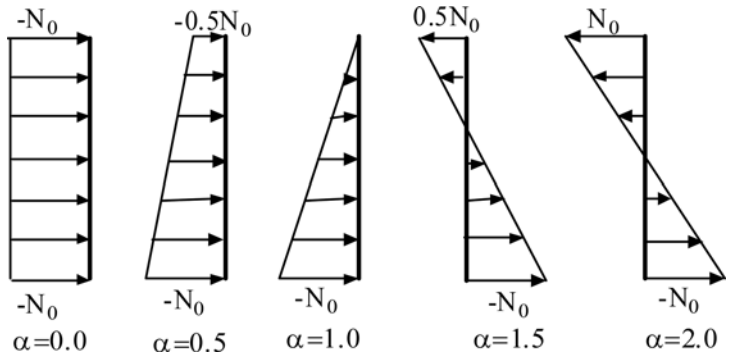

Fig. 2 Example of in-plane loading N_x along the edge $x = 0$

Table 1 Non-dimensional buckling load N_{cr}^{*} for different loading cases and aspect ratios

a/b	α	N_{cr}^{*}		
		This Study	Kang and Leissa	Ratio
1	0.00	39.42	39.48	0.998
1	0.50	52.42	52.49	0.999
1	1.00	76.99	77.08	0.999
1	1.50	133.15	132.00	1.009
1	2.00	250.79	253.00	0.991
2	0.00	39.43	39.48	0.999
2	0.50	52.43	52.82	0.993
2	1.00	77.00	77.21	0.997
2	1.50	133.18	132.63	1.004
2	2.00	235.16	235.70	0.998
3	0.00	39.42	39.48	0.999
3	0.50	52.42	52.35	1.001
3	1.00	76.99	76.77	1.003
3	1.50	133.17	132.34	1.006
3	2.00	237.26	237.67	0.998

The buckling load of rectangular plates is presented in a normalized form as follows

$$N^{*} = \frac{N_{o}^{*}}{N_{cr}^{*}} \tag{10}$$

where N_{o}^{*} and N_{cr}^{*} are the non-dimensional elastic critical load of the plate with and without a cutout, respectively. A number of plates with different loading cases (α ranging from 0 to 2), normalized hole sizes (d/b ratios ranging from 0.0 to 0.7), the different locations of cutout (x_{edge}/b ranging from 0.5 to 2) and aspect ratios (a/b ranging from 1 to 4) were analyzed by using the finite element package in ANSYS. Fig. 3 shows the variation in the buckling load ratios N^{*} as the normalized hole size (d/b) for various loading conditions.

Close observation of Fig. 3(c) shows clearly that the presence of a small hole (i.e., $d/b = 0.1$ and 0.2) has no considerable effect on the buckling load ratio of the rectangular plate. However, moving the holes with large diameter ($d/b = 0.5$-0.7) along the x-axis causes a significant variation on buckling load ratios N^{*}, this effect is even more significant for the compression loading cases. For example the plate having a circular hole, whose center is at the middle of the plate, can buckle at loads higher than the buckling load for corresponding plates without a cutout. Even though this behavior is somewhat counterintuitive at first glance, this has been studied for many years and experimentally verified for isotropic plates (Komur and Sonmez 2008, El-Sawy and Namzy 2001). The buckled mode shape of the plate may be used to explain such behavior. A solid plate subjected to compression buckles in a double half waves, but the presence of large hole at the middle of the plate changes from double half waves to three half waves. The presence of large hole changes the buckling mode shape of the plate having $a/b = 2$. This makes the buckled loads of the rectangular plates with aspect ratio of 2 larger than Ncr for the compression loading cases. All the buckling

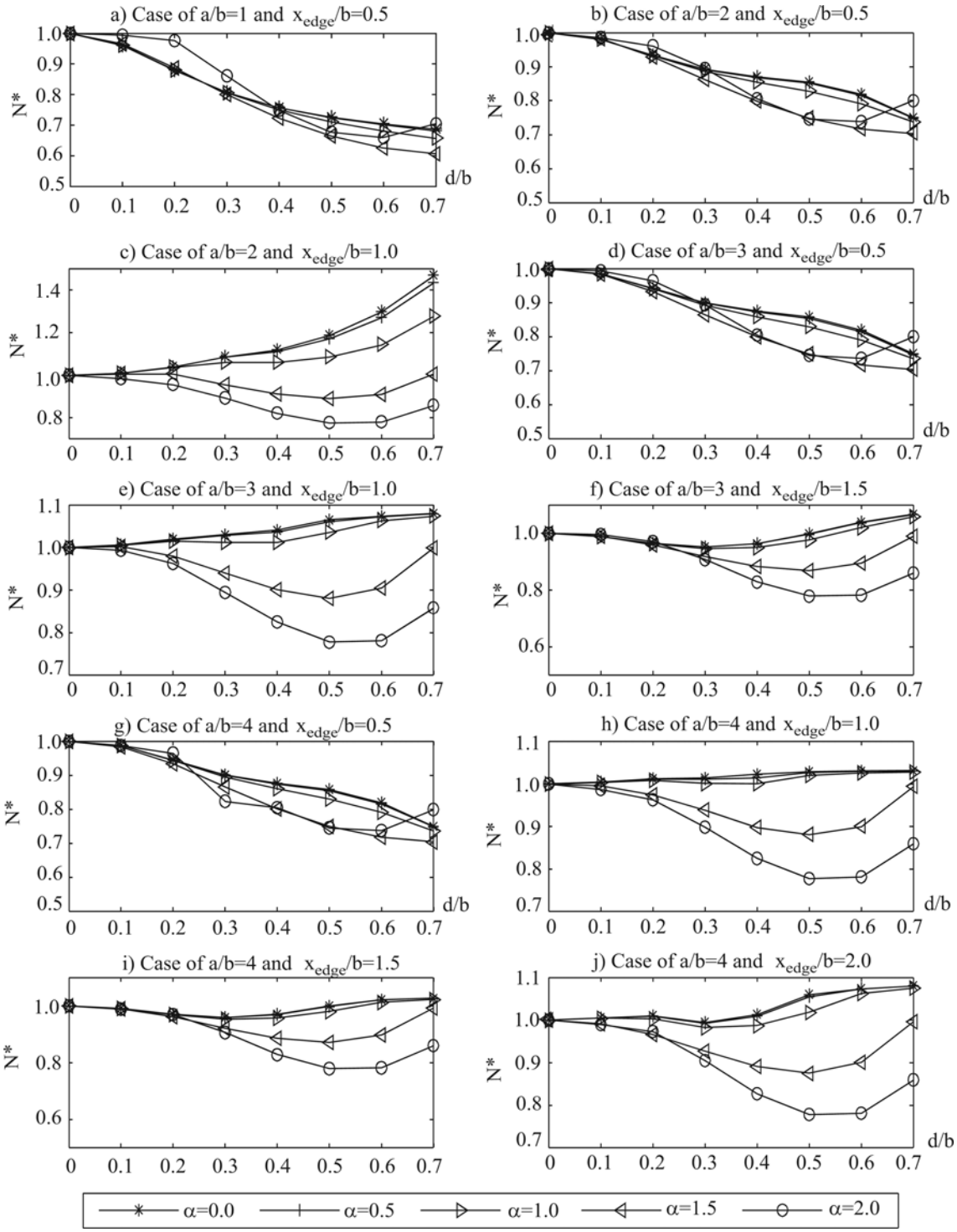

Fig. 3 Buckling load ratios N^* of plates with a cutout

load ratios are less than one for the bending loading cases, because there is no change in the mode shapes while the hole is moved along the x-axis.

5. Artificial natural networks

5.1 Background

ANN is an information processing paradigm that has broad applicability to real world problems including pattern recognition, identification, classification and control systems. It is based on an artificial representation of the human brain that tries to simulate its learning process. The term "artificial" means that neural nets are implemented in computer programs that are able to handle the large number of necessary calculations during the learning process. ANNs consist of very simple and highly interconnected processors called neurons or processing elements. The neurons are connected to each other by weighted links over which signals can pass. Each neuron receives multiple inputs from other neurons in proportion to their connection weights and generates a single output, which may be propagated to a number of other neurons.

The multilayer perceptron (MLP) is by far the most well known and most popular ANN among all the existing ANN paradigms (Rumelhart and MacClelland 1986). It consists of at least three or more layers, which comprises an input layer, an output layer and a number of hidden layers. Each neuron in one layer is connected to the neurons in the next layer and there are no connections among the units of the same layer (Kasabov 1996, Haykin 1999). The number of neurons in each layer may vary depending on the problem. The layers between the input layer and output layer are referred to as hidden layers. MLPs have been applied successfully to many complex real-world problems consisting of non-linear decision boundaries. Three-layer MLPs have been sufficient for most of these applications (Omondi and Rajapakse 2006).

Back Propagation Algorithm (BPA) is one of the most famous training algorithms for the MLP to its success from both simplicity and applicability viewpoints. It is a gradient descent technique to minimise the error through a particular training pattern in which it adjusts the weights by a small amount at a time. The algorithm consists of two phases: Training phase and recall phase. In the training phase, first, the weights of the network are randomly initialized. Then, the output of the network is calculated and compared to the desired value. In sequel, the error of the network is calculated and used to adjust the weights of the output layer. In a similar fashion, the network error is also propagated backward and used to update the weights of the previous layers.

A number of approaches for training neural networks are used. Most of them fall into two classes: i) unsupervised and ii) supervised learning. Unsupervised system must organize itself by internal criteria and local information designed into the network. Learning process is carried out without being taught. In this class, only the input samples are used to train the network. On the other hand, supervised learning algorithms may change weights of neurons according to the inputs/outputs samples. After a network has established its input/output mapping with a defined minimum error value, the training task has been completed. In sequel, the network can be used in recall phase in order to find the outputs for new inputs. An important factor is that the training set should be comprehensive and cover all the practical areas of applications of the network. Therefore, the proper selection of the training sets is critical to the good performance of the network (Zilouchian and Jamshidi 2001).

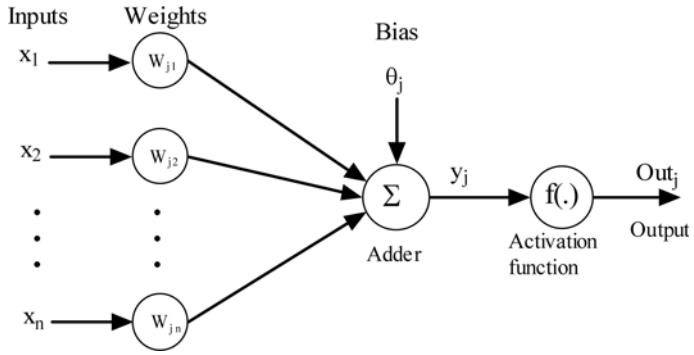

Fig. 4 Basic elements of an artificial neuron

In Fig. 4, various inputs to the network are represented by the mathematical symbol x_i. Each of these inputs is multiplied by a connection weight. These weights are represented by w_{ji}. In the simplest case, these products are summed, fed through a transfer function to generate a result, and then output. This figure also includes the bias θ_j, which has the effect of lowering or increasing the net input of the activation function (Haykin 1999).

The relation between the input x_i, and the output signal Out_j of a single neuron is formulated as follows

$$Out_j = f\left(\sum_{i=1}^{n} w_{ij}x_i + \theta_j\right) \quad j = 1, 2, \ldots, n \tag{11}$$

where Out_j is the output of the jth neuron. $f(.)$ is a called an "activation" or "transfer" function, which could be a sigmoid or hyperbolic tangent function (Haykin 1999).

The training of the network is accomplished by adjusting the weights and is carried out through a large number of training sets and training cycles (epochs). The goal of the training procedure is to find the optimal set of weights, which in an ideal case would produce the right output for any input and minimize global error between the model output and the target output. The training is carried out until the global error, such as the absolute fraction of variance (R^2), the root mean square error (RMS), or the mean absolute error (MAE), gets to an acceptable level. Global errors are given by the following equations

$$R^2 = 1 - \frac{SSE}{\sum_{i=1}^{n}\sum_{j=1}^{m}(T_{ij})^2} \tag{12}$$

$$RMS = \sqrt{\frac{SSE}{n \cdot m}} \tag{13}$$

$$MAE = \frac{100}{n \cdot m}\sum_{i=1}^{n}\sum_{j=1}^{m}\left|\frac{T_{ij} - Out_{ij}}{T_{ij}}\right| \tag{14}$$

where m is the number of neurons in the output layer and n is the number of samples. T_{ij} and Out_{ij} are the actual (target) values and the output of neural network values, respectively. SSE is the sum of the square of errors, defined as

$$SSE = \sum_{i=1}^{n}\sum_{j=1}^{m}(T_{ij} - Out_{ij})^2 \tag{15}$$

5.2 Development of ANN model

A review of different ANN models is found in several papers and books (e.g., Veelenturf 1995, Haykin 1999, Pala 2006, Elhatip and Komur 2008). Among the various types of ANN, the feed-forward or multilayer perceptron neural network is widely used for function approximation, with numerous successful applications in almost every scientific and engineering domain (Pu and Mesbahi 2006). In the training process of the feed-forward algorithm, the input information is propagated forward through the network, while the output error is back-propagated through the network for updating the weights. The back-propagation algorithm can speed up and stabilize the convergence during training. In this study, the multilayer feed-forward network trained by supervised learning was chosen. This model also uses a scaled conjugate gradient training algorithm (SCGA), which avoids a time-consuming line search per learning iteration. A sigmoid function has been used as an activation function and approximately 4000 epochs have been used in the training of the ANN model. In this study the built in function which is available in Matlab ANN toolbox is used for ANN applications. An interface developed to call these toolbox functions when they are needed.

The ANN model was trained and tested by means of the previously described results obtained by finite element analysis. Randomly selected 320 FEM results out of 400 were used to train the network while the rest of the data was used for testing the model. Input and output data were normalized by using the normalization values given in Table 2, since the sigmoid function having asymptotic limits of [0, 1] was used in training the ANN model. Table 2 also gives the range of the input parameters in which the input data are valid.

The number of neurons in the input layer is set to 4, namely the aspect ratio (a/b), hole size (d/b), loading case (α), and the location of circular hole (x_{edge}/b). The number of neurons in the output layer is 1, which returns the elastic buckling load of the perforated plate. The number of neurons in the hidden layer has a direct effect on the model quality in terms of accuracy; hence, selecting the number of neurons in the hidden layer is the key issue in the development of an ANN model (El-Kassas *et al.* 2002). Unfortunately, there is no rule of thumb to determine the number of the hidden layers and the neurons in these layers. In practice, a trial-and-error procedure must be carried out (Haykin 1999, Guzelbey *et al.* 2006). In order to determine the most appropriate ANN model, several multi-layer perceptron architectures with various numbers of hidden layers and nodes were developed and tested in this study. The most appropriate ANN model is selected based on the performance of both training and testing sets in terms of the RMS Errors. A number of ANN models having one and two hidden layers with different number of neurons are developed and the corresponding RMS errors are given in Fig. 5 and Fig 6, respectively. In Fig. 6, x-axis is label as

Table 2 The range of inputs and output parameters and normalized values

Parameters	Range of Values	Normalization Value
Aspect Ratio, a/b	1.0-4.0	4
Hole size, d/b	0.0-0.7	0.7
Loading case, α	0.0-2.0	2
Location of Hole, x_{edge}/b	0.5-2.0	2
Buckling load, N_{cr}^{*}	0.00-300.00	300.00

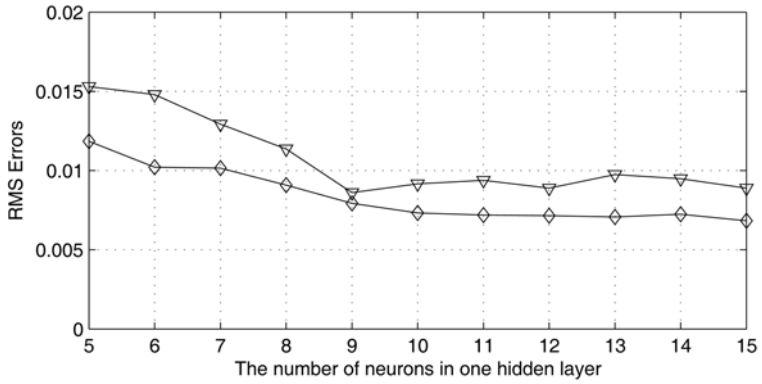

Fig. 5 Effect of the neuron number for a single hidden layer case

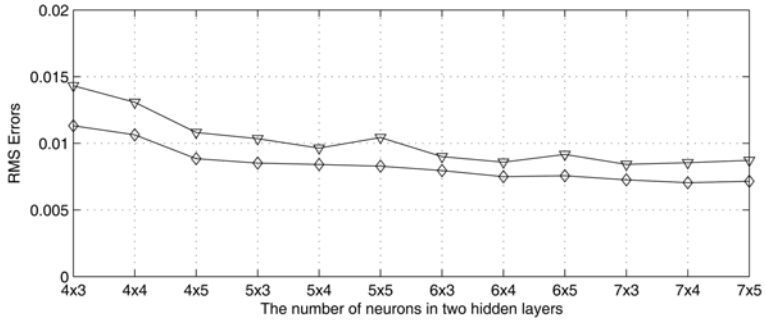

Fig. 6 Effect of the neuron number for two hidden layer case

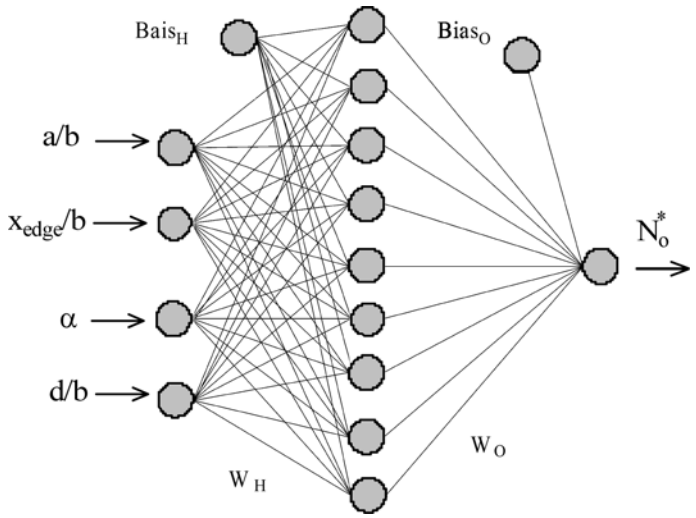

Fig. 7 The architecture of the proposed ANN model

AxB on which A and B denote the neurons in the first and second hidden layer, respectively. As can be seen from Figs. 5 and 6, the comparison of the performance of the ANN models with both one and two hidden layers revealed the fact that the one hidden layer model with 9 neurons resulted

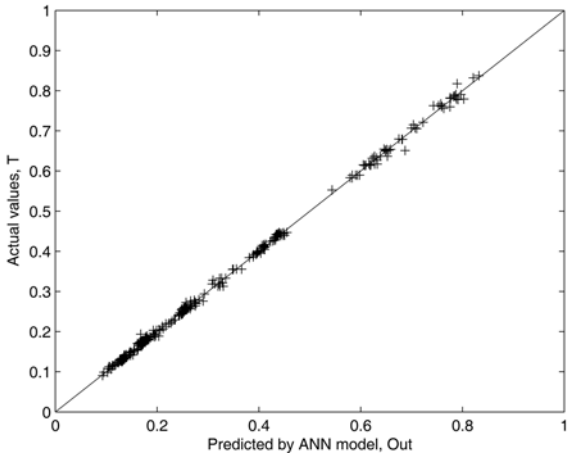

Fig. 8 Performance of the ANN model for the training set

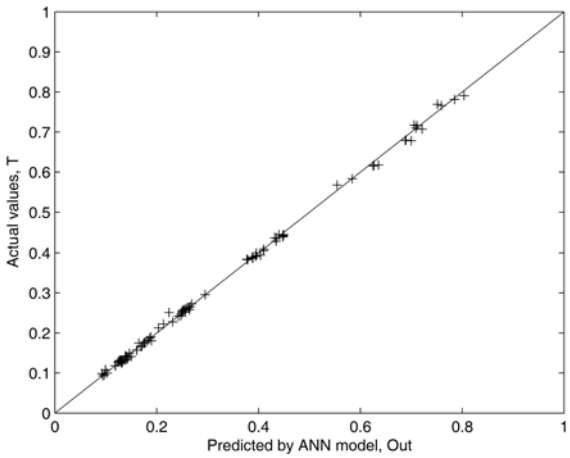

Fig. 9 Performance of the ANN model for the test set

Table 3 Statistical parameters for the ANN used for elastic buckling

	Training Set	Test Set
R^2	0.99973	0.99965
RMS	0.006175	0.006926
MAE	1.67	2.01

in better model accuracy. Consequently, the ANN model is selected as having 4 neurons in input layer, 9 neurons in first hidden layer and 1 neuron in output layer to define the buckling load of elastic perforated plates. The ANN model used in this study is depicted in Fig. 7.

Fig. 8 shows the correlation of predicted values (by ANN model) and actual values (obtained from finite element analysis) when the 320 samples were used for training the network. The network predicted them very well. Fig. 9 shows the predicted and actual values of the buckling load when 80 samples that were not used for training were used for testing the network. The training and test errors are given in Table 3. The R^2 values were found to be 99.97% and 99.97% and the mean absolute error was 1.67% and 2.01% for the train and test sets of the buckling load, respectively. It was observed from the results that the network can predict the elastic buckling load of plates within a very small error margin. This indicates that the developed ANN model is quite accurate.

5.3 Explicit formulation of the ANN model

Although ANN has been employed successfully to solve complex engineering problems, its capacity to establish a functional relationship between input and output data has not been thoroughly investigated (Pu and Mesbahi 2006, Pala 2006). The functional relationship between input parameters (aspect ratio, loading case, location and size of hole) and the output parameter (elastic buckling load) was derived based on the trained ANN model. The elastic buckling of plate N_o^* was obtained in the functional form as

$$N_o^* = \frac{300.00}{1 + e^{-(W_o * Out_h + 6.258)}} \tag{16}$$

$$W_o = \{2.331 \ \ -4.932 \ -2.284 \ -1.164 \ 2.583 \ -8.165 \ -1.122 \ 5.230 \ -303\} \tag{17}$$

Where 6.258 is the bias value and W_o is the weight matrix of 9 neurons between the hidden layer and the output layer. Out_h is the output vector of 9 neurons in the hidden layer, which is expressed as

$$Out_h = \left\{ \frac{1}{1+e^{-y_1}} \ \ \frac{1}{1+e^{-y_2}} \ \ \frac{1}{1+e^{-y_3}} \ \cdots \ \frac{1}{1+e^{-y_9}} \right\}^T \tag{18}$$

Where $y_1, y_2, y_3, y_4, y_5, y_6, y_7, y_8$ and y_9 are the weighted inputs of the neurons in the hidden layer. They are obtained by using Eqs. (19)-(23)

$$Y_h = W_h \times X + \theta_h \tag{19}$$

$$Y_h = \{y_1 \ \ y_2 \ \ y_3 \ \ y_4 \ \ y_5 \ \ y_6 \ \ y_7 \ \ y_8 \ \ y_9\}^T \tag{20}$$

$$W_h = \begin{bmatrix} 2.045 & 2.106 & -0.666 & -0.142 & 2.416 & 0.093 & -2.153 & 7.176 & 0.883 \\ -0.698 & 3.069 & -0.667 & 0.240 & 4.450 & 0.158 & -17.409 & 2.863 & -0.513 \\ -9.029 & -1.870 & -2.907 & 7.204 & -3.683 & -5.428 & -1.068 & 0.437 & -7.682 \\ -5.356 & -1.228 & -0.001 & -9.529 & -1.446 & 1.919 & 3.335 & -1.165 & -7.083 \end{bmatrix}^T \tag{21}$$

$$\theta_h = \{12.865 \ \ 0.436 \ \ 2.946 \ \ -6.607 \ \ 0.827 \ \ 5.986 \ \ 3.5226 \ \ 1.181 \ \ 14.138\}^T \tag{22}$$

$$X = \left\{ \frac{a/b}{4} \ \ \frac{x_{edge}/b}{2} \ \ \frac{\alpha}{2} \ \ \frac{b/d}{0.7} \right\}^T \tag{23}$$

W_h and θ_h are the weight matrices and bias value vector of input variables in the input layer to neurons in the hidden layer. X is the normalized input vector. It should be noted that the proposed NN model be valid within the ranges of variables given in Table 2.

6. Verification of the proposed formula

The explicit formula in Eq. (16), which was proposed for the calculation of elastic buckling load of perforated plates, can be verified by comparing the ANN results with those available in the literature, namely from Kang and Leissa (2005) and El-Sawy and Nazmy (2001). Kang and Leissa (2005) investigated the linearly varying loading on the buckling load of the solid plates by using an exact solution procedure based on the infinite power series. El-Sawy and Nazmy (2001) used the finite element method to obtain the elastic buckling load of perforated plates subjected to uniformly distributed force. The results are given in Tables 4 and 5. For verification, a comparison between the two results and statistical values such as MAE and the maximum absolute errors are also given in Tables 4 and 5. It can be seen that nearly every prediction is accurate to within less than 5 percent. The maximum deviation takes place when the aspect ratio is 2.30, even though this aspect

Table 4 Compression of proposed ANN formulation and Kang and Leissan's results

a/b	x_{edge}/b	α	d/b	Kang (2005)	ANN-Formula	Ratio
2.30	1.15	0.00	0.00	39.48	38.92	1.0144
2.30	1.15	0.50	0.00	52.49	50.30	1.0435
2.30	1.15	1.00	0.00	77.08	75.60	1.0196
2.30	1.15	1.50	0.00	132.00	133.38	0.9897
2.30	1.15	2.00	0.00	235.70	240.51	0.9800
1.00	0.50	2.00	0.00	252.00	249.74	1.0090
1.00	0.50	1.33	0.00	108.70	106.80	1.0178
1.00	0.50	1.00	0.00	77.10	75.95	1.0151
1.00	0.50	0.80	0.00	65.09	64.61	1.0074
1.00	0.50	0.67	0.00	58.86	58.67	1.0032
1.50	0.75	2.00	0.00	238.00	244.41	0.9739
1.50	0.75	1.33	0.00	113.3	112.57	1.0065
1.50	0.75	1.00	0.00	82.59	80.83	1.0218
1.50	0.75	0.80	0.00	70.2	68.40	1.0263
1.50	0.75	0.67	0.00	63.64	62.05	1.0256
Maximum absolute error: 4.17						
MAE: 1.75						

Table 5 Compression of proposed ANN formulation and El-Sawy and Nazmy's results

a/b	x_{edge}/b	α	d/b	El-Sawy (2001)	ANN-Formula	Ratio
1.00	0.50	0.00	0.20	34.84	35.15	0.9912
1.00	0.50	0.00	0.60	27.63	28.38	0.9736
2.00	0.50	0.00	0.10	38.69	38.66	1.0008
2.00	1.00	0.00	0.50	46.88	46.56	1.0069
3.00	0.50	0.00	0.40	34.54	33.64	1.0268
3.00	1.00	0.00	0.60	42.44	44.42	0.9554
4.00	0.50	0.00	0.20	37.50	36.95	1.0149
4.00	1.00	0.00	0.50	40.66	41.20	0.9869
3.00	1.50	0.00	0.65	41.65	41.73	0.9981
4.00	1.50	0.00	0.60	40.47	40.68	0.9948
4.00	2.00	0.00	0.45	39.48	40.37	0.9780
Maximum absolute error: 4.67						
MAE: 1.58						

ratio was not used in training the ANN model. The prediction of the buckling load had a very high accuracy, mostly within ±2 percent.

7. Conclusions

The elastic buckling load of simply supported perforated rectangular plates subjected to linearly varying loading has been obtained by using the finite element method. The results were then used to train and test a multilayer, feed-forward neural network using the supervised learning method to predict the elastic buckling of perforated plates in terms of aspect ratio, size, and location of cutout and load cases. An ANN model that had one hidden layer with nine neurons was chosen. The model was shown to be capable of providing accurate estimates of the elastic buckling load of plates. Based on the trained model, an ANN-based formula to predict the elastic buckling load of perforated plates was presented. The formula presented was verified using results obtained from the literature to check its accuracy in predicting the buckling load of perforated plates. It was found that the proposed formula gives very accurate predictions, mostly within ±2 percent error.

ANN is generally an easy-to-use tool to solve engineering problems, but it may also be used in establish a mathematical expression between inputs and output results by means of the weight and bias terms of neurons based on the activation function. In this study, an ANN-based formula is presented. The proposed formula does not require rigorous mathematical computations and a single formula covers different loading patterns, sizes and locations of the hole, and different aspect ratios of the plates.

The method presented here can be improved by including nonlinear behavior of perforated plates. In order to so, a series of experimental and analytical studies should be performed to obtain the necessary data set for training the model.

Acknowledgements

The authors would like to express their thanks to Karadeniz Technical University for access to their ANSYS software.

References

ANSYS (2005), User Manual, Version 10.0, ANSYS, Inc.

Brown, C.J. and Yettram, A.L. (1986), "The elastic stability of square perforated plates under combination of bending, shear and direct load", *Thin Wall. Struct.*, **4**(3), 239-246.

Brown, C.J., Yettram, A.L. and Burnett, M. (1987), "Stability of plates with rectangular holes", *J. Struct. Eng.*, ASCE, **113**(5), 1111-1116.

Brown, C.J. (1990), "Elastic buckling of perforated plates subjected to concentrated loads", *Comput. Struct.*, **36**(6), 1103-1109.

Brush, D.O. and Almroth, B.O. (1975), *Buckling of Bars, Plates and Shells*, McGraw-Hill, Inc.

Cevik, A. and Guzelbey, I.H. (2007), "A soft computing based approach for the prediction of ultimate strength of metal plates in compression", *Eng. Struct.*, **29**, 383-394.

Chajes, A. (1974), *Principle of Structural Stability Theory*, Prentice-Hall, Inc.

Cook, M.E., Malkus, D.S. and Plesha, M.E. (1989), *Concepts and Applications of Finite Element Analysis*, 3nd ed. John Wiley & Sons, USA, 441-444.

Elhatip, H. and Komur, M.A. (2008), "Evaluation of water quality parameters for the Mamasin dam in Aksaray in the Anatolian part of Turkey by means of artificial neural networks", *Environ. Geol.*, **53**, 1157-1164.

El-Kassas, E.M.A., Mackie, R.I. and El-Sheikh, A.I. (2002), "Using neural networks to predict the design load of

cold-formed steel compression members", *Adv. Eng. Softw.*, **33**, 713-719.
El-Sawy, K.M. and Nazmy, A.S. (2001), "Effect of aspect ratio on the elastic buckling of uniaxially loaded plates with eccentric holes", *Thin Wall. Struct.*, **39**, 983-998.
El-Sawy, K.M., Nazmy A.S. and Martini M.I. (2004), "Elasto-plastic buckling of perforated plates under uniaxial compression", *Thin Wall. Struct.*, **42**, 1083-1101.
Guzelbey, H., Cevik, A. and Gogus, M.T. (2006), "Prediction of rotation capacity of wide flange beams using neural networks", *J. Construct. Steel Res.*, **62**, 950-961.
Haykin, S. (1999), *Neural Networks: A Comprehensive Foundation*, Pearson Education, Inc, 2nd ed.
Kang, J.H. and Leissa, A.W. (2005), "Exact solutions for the buckling rectangular plates having linearly varying in-plane loading on two opposite simply supported edges", *Int. J. Solids Struct.*, **42**, 4220-4238.
Kasabov, N.K. (1996), *Foundations of Neural Networks, Fuzzy Systems, and Knowledge Engineering*, MIT Press, Cambridge, MA.
Komur, M.A. and Sonmez, M. (2008), "Elastic buckling of perforated plates subjected to linearly varying in-plane loading", *Struct. Eng. Mech.*, **28**(3), 353-356.
Komur, M.A. and Sonmez, M. (2008), "Elastic buckling of rectangular plates under linearly varying in-plane normal load with a circular cutout", *Mech. Res. Commun.*, **35**, 361-371.
Komur, M.A. and Sonmez, M. (2005), "Application of artificial neutral network approach on elastic buckling analysis of rectangular plates", XIV. National Mechanic Symposium, September 12-16, Mustafa Kemal University, Hatay. (in Turkish)
Leissa A.W. and Kang J.H. (2002), "Exact solutions for vibration and buckling of an SS-C-SS-C rectangular plate loaded by linearly varying in-plane stresses", *Int. J. Mech.* Sci., **44**, 1925-1945.
Omondi, A.R. and Rajapakse, J.C. (2006), *Fpga Implementations of Neural Networks*, Springer, Netherlands.
Pala, M. (2006), "A new formulation for distortional buckling stress in cold-formed steel members", *J. Construct. Steel Res.*, **62**, 716-722.
Pu, Y. and Mesbahi, E. (2006), "Application of artificial neural networks to evaluation of ultimate strength of steel panels", *Eng. Struct.*, **28**, 1190-1196.
Rumelhart, D.E. and MacClelland, J.L. (1986), *Parallel Distributed Processing: Explorations in the Microstructure of Cognition*. MIT Press, Cambridge, MA.
Shanmugam, N.E., Thevendran, V. and Tan, Y.H. (1999), "Design formula for axially compressed perforated plates", *Thin Wall. Struct.*, **34**(1), 1-20.
Shakerley, T.M. and Brown C.J. (1986), "Elastic buckling of plates with eccentrically positioned rectangular perforations", *Int. J. Mech. Sci.*, **38**(8-9), 825-838.
Timoshenko, S.P. and Gere, J.M. (1961), *Theory of Elastic Stability*, McGraw-Hill, Second ed., New York.
Veelenturf, L.PJ. (1995), *Analysis And Application of Artificial Neural Networks*, Prentice, Hall, Ltd.
Zilouchian, A. and Jamshidi, M. (2001), *Intelligent Control Systems using Soft Computing Methodologies,* CRC Press.